Scientific paper

Synthesis, Crystal Structure and Physico-chemical Properties of 3,3'-[(4-hydroxyphenyl)methyl] bis-(4-hydroxy-*2H*-chromen-2-one)

Denitsa Elenkova,[1] Bernd Morgenstern,[2] Ilia Manolov[3] and Maria Milanova[1,*]

[1] *University of Sofia "St. Kliment Ohridski", Faculty of Chemistry and Pharmacy, Department of Inorganic Chemistry, 1, J. Bourchier, 1164 Sofia, Bulgaria*

[2] *Laboratory for Inorganic and Coordination Chemistry, Saarland University, 66123 Saarbrücken, Germany*

[3] *Medical University, Faculty of Pharmacy, Department of Pharmaceutical Chemistry, 2 Dunav Str., Sofia, Bulgaria*

* *Corresponding author: E-mail: nhmm@chem.uni-sofia.bg*
tel. +3592 8161322

Received: 11-03-2014

Abstract

The compound 3,3'-[(4-Hydroxyphenyl)methyl]bis-(4-hydroxy-2*H*-chromen-2-one) was synthesized by the Knoevenagel reaction. Crystals, suitable for X-ray data collection, were grown by slow evaporation from an ethanol solution. The product 3,3'-[(4-Hydroxyphenyl)methyl]bis-(4-hydroxy-2*H*-chromen-2-one) · ethanol crystallizes in the monoclinic system, space group $P2_1/n$. The ultraviolet/visible absorption spectra in different solvents were recorded. Sensitivity of the compound to solvent polarity and hydrogen bonding with protic (ethanol, H_2O) and aprotic (dimethylsulfoxide, acetonitrile) solvents was detected. Based on ^{1}H-NMR spectroscopy as well as on potentiometric and UV/vis titration experiments the acid dissociation constants for 3,3'-[(4-Hydroxyphenyl)methyl]bis-(4-hydroxy-2*H*-chromen-2-one) were estimated.

Keywords: 4-hydroxy-bis-coumarins, X-ray diffraction, ^{1}H-NMR spectroscopy, UV-Vis spectrometry, potentiometric titration

1. Introduction

1. 1. The Coumarins

The benzo-α-pyrones, or coumarins, are a group of compounds consisting of fused pyrone and benzene rings, with the pyrone carbonyl group at position 2 (IUPAC name *2H*-chromen-2-one, also known as 1-benzopyran-2-one).[1] They are important compounds among the natural products and in the organic synthesis. Recently, coumarin derivatives attracted scientific interest because of the interesting properties these compounds possess, namely bioactivity and physiological properties;[2–15] their optical properties allow applications as laser dyes, phosphorescent[16] and photochemical materials,[17,18] as well as probes for heterogeneous systems using fluorescence spectroscopy.[1] They are synthesized by different methods including condensation processes,[6–15,19] recently by environmentally friendly process using sulfated titania catalyst,[20] phosphotungstic acid as a catalyst.[21] The crystal structure of some of them was solved and reported in the literature,[22–27] but there is not available crystal data about the compound in the work presented. The coumarin derivatives have been successfully tested as ligands for synthesis of complexes with lanthanoids;[25, 28, 29] the complexes obtained have shown optical,[25] and biological activity,[28–31] improved in comparison with the ligands themselves. The derivatives of 4-hydroxy-bis-coumarins are interesting because they have at least 2 OH groups in the structure and are therefore polyprotic organic acids. One of the procedures used for synthesis of Ln(III) complexes with 4-hydroxy-biscoumarins[28,30,31] as well as with other coumarin derivatives[29] includes formation of a sodium salt of the coumarin in H_2O solution with sodium hydroxide, usually at stoichiometric ratios ligand/NaOH. Deprotonation of OH groups of the ligand can be expected. The studied

compound has a very low solubility in water. Solvents different than pure water have to be found in order to be able to determine the pK_a via potentiometric titration. Systems such as DMSO/H_2O or C_2H_5OH/H_2O may be suitable. The stability of bis-coumarins in such systems is important. A convenient method to get information about the behavior of bis-coumarins in different solvents is UV-vis spectroscopy. Some of the first UV absorption spectra of a series of mono-coumarin derivatives have been determined in order to help the identification of unknown fractions isolated from roots.[32] It has been found that the chemical composition,[33,34] the substitutes,[35,36] and the pH value of the solvent used[32] can have an important influence on the shape of the absorption spectra.

1. 2. The Contribution of the Work Presented

The 4-hydroxy-bis-coumarins described are derivatives of 3,3'-benzylidene bis(4-hydroxy-2*H*-1-benzopyran-2-one) or 3,3'-phenylmethyl bis-(4-hydroxy-2*H*-chromen-2-one) (Figure 1) with substitutes on m- or p-position by OH, -NO_2, or -Cl.

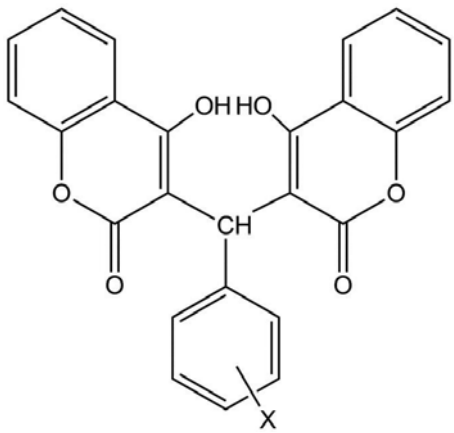

Figure 1. Chemical formula of 3,3'-(phenylmethyl)bis(4-hydroxy-2*H*-chromen-2-one). For L10, X = -OH (p), and for L16 X_1 = Cl (p), X_2 = NO_2 (m).

The substitute influences the properties of the respective coumarin, as shown by investigations on some mono-coumarins[35,36] as well as by our experiments. The work presents results on investigation of 3,3'-[(4-Hydroxyphenyl)methyl]bis-(4-hydroxy-2*H*-chromen-2-one) (L10), which is synthesized as a powder sample by the synthetic procedure in [11]. The single crystals obtained gave a chance to elucidate the crystal structure of the compound L10 for a first time. Based on the crystal structure and the information it gave, speculations were made for the bonds between the molecules.

The behavior of 3,3'-[(4-Hydroxyphenyl)methyl] bis-(4-hydroxy-2*H*-chromen-2-one) (L10) in protic and aprotic solvents was investigated as well as its optical properties in solid state. In order to support the eliucidation of the properties of L10, some data obtained for 3,3'-[(4-Chloro-3-nitrophenyl)methyl]bis-(4-hydroxy-2*H*-chromen-2-one), (L16) and 3,3'-[(4-Chloro-phenyl)methyl] bis-(4-hydroxy-2*H*-chromen-2-one), (L15) are given as well. The combination of several techniques (^{1}H-NMR spectroscopy, potentiometric and UV-Vis titrations) was used to estimate the pKa of a compound which is with a low stability with the time in some solutions.

2. Experimental

2. 1. Materials

4-Hydroxycoumarin, 4-hydroxybenzaldehyde, glacial acetic acid and ethanol were purchased from Merck and were used without further purification. Melting points were measured in open capillary tubes on a Büchi 535 melting point apparatus.

2. 2. Synthetic Procedure

The compound 3,3'-[(4-Hydroxyphenyl)methyl]bis-(4-hydroxy-2*H*-chromen-2-one), $C_{25}H_{16}O_7$ (L10), was synthesized by reaction of 4-hydroxycoumarin (3.24 g, 20 mmol) and 4-hydroxybenzaldehyde (1.22 g, 10 mmol) (molar ratio 2:1) in 30 mL glacial acetic acid at reflux for 7 h until the appearance of an insoluble product. After cooling, the product was filtered and recrystallized from ethanol. The yield was 3.20 g (75%), m.p. 212–214 °C. TLC: R_f = 0.94 (hexane:chloroform:acetone = 10:10:4). The successful preparation of the powdered sample was confirmed by elemental analysis ($C_{25}H_{16}O_7$ calc. C = 70.09, H = 3.74%; found: C = 70.31, H = 3.89%), IR spectroscopy (recorded in nujol; peaks at 1668, 1609, 1091, 764 cm^{-1}), ^{1}H NMR (in DMSO-d_6): peaks at 6.27 (s, 1H, CH), 6.65–7.38 (m, 12H, Ar-H) and mass spectroscopy (peaks observed at m/e = 428 (5), 335 (8), 265 (7), 162 (100), 120 (71), 92 (78), 63 (13)).

Crystals, suitable for X-ray data collection, were grown by slow evaporation from an ethanol solution. There was not enough of them for elemental analysis.

2. 3. Methods for Characterization

X-Ray Diffractometry. Measurements were made at 123 K on a Bruker X8 Apex-II, Nonius Kappa CCD diffractometer using graphite monochromated Mo-K_α radiation (λ = 0.71073 Å). The structure was refined by full–matrix least–squares techniques on F^2.[37] The conditions of X-ray analysis together with the crystallographic data are given in Table 1. The data set was semi-empirically corrected for absorption effects (multi-scan).[41] All non-hydrogen atoms were refined using anisotropic displacement parameters. For C-bonded hydrogen atoms a ri-

ding model was used, whereas the O-bonded hydrogen atoms were refined using isotropic displacement parameters with $1.5 \times U_{eq}$ of the pivot atom and restraints of 0.84 for the corresponding OH distances.[42]

Infrared spectroscopy (IR). Infrared spectral analysis was carried out on a Shimadzu FTIR-8101 M IR-spectrometer.

Mass spectroscopy. Mass spectra were recorded on a JEOL JMS D 300 double focusing mass spectrometer coupled to a JMA 2000 data system. The compound was introduced through a direct inlet probe, heated from 50 °C to 400 °C at a rate of 100 °/min. The ionization current was 300 mA, the accelerating voltage 3 kV and the chamber temperature 150 °C.

NMR spectroscopy. ^{1}H NMR spectra were recorded at ambient temperature on a Bruker Avance II +600 (600 MHz) in [D6]-DMSO (for the synthesized sample) and a Bruker 250 WM (250 MHz) spectrometer in [D_6]-acetone (for the other measurements). The ^{1}H-NMR titration experiments were performed on a Bruker DRX Avance 400 MHz NMR spectrometer. The particular pH* was adjusted with aqueous solutions of NaOD and DCl in a mixture of D_2O/DMSO. (The term pH* refers to the direct pH-meter reading (Metrohm 713 pH meter) of the D_2O/d_6-DMSO mixtures. A pH Ag/AgCl-electrode (Metrohm) was calibrated with three aqueous (H_2O) buffer solutions). Chemical shifts are given in ppm relative to D_4-sodium (trimethylsilyl)propionate as internal standard ($\delta = 0$ ppm).

Photoluminescence measurements were made on a Cary Eclipse spectrometer using a xenon lamp as the excitation source.

UV-Vis absorption spectroscopy. Evolution 300 UV-Vis spectrometer (Thermo Scientific) was used for measuring the absorption of the samples in the range 200–900 nm.

Potentiometric measurements. The pK_a values of the investigated ligands were determined in mixtures of DMSO/H_2O (50 mL) ensuring a mole fraction for DMSO of 0.2 and an ionic strength of 0.1 M KCl using a Metrohm 665 piston burette, a Metrohm 713 pH/mV meter and a glass electrode with an incorporated Ag/AgCl reference. A constant temperature of the solution was guaranteed using a Lauda ecoline103 thermostat. A solution of KOH, based on 0.1 M KOH (Titrisol, Merck) and a given proportion of DMSO resulting in a mole fraction of 0.2 was used as a titrant. The mole fraction of 0.2 of the DMSO/H_2O mixture was prepared using the values for the partial molar volumes of the two components at 25°C.[38] To ensure complete equilibration and to guarantee that no decomposition of the individual ligands has been occurred, back titrations (0.1 M HCl/DMSO; $x_{DMSO} = 0.2$) were performed.

Calculations of the protonation constants. The pK_a values were evaluated using HYPERQUAD2008.[39] The protonation constants were calculated as concentration constants, and pH was defined as $-\log[H^+]$. A fixed value for the ionization constant of 15.59 for the investigated mole fraction was used,[40] and the total concentrations of the ligands were always treated as fixed values.

3. Results and Discussion

3. 1. X-ray Diffraction Analysis

Single crystals suitable for crystal structure analysis were grown by slow evaporation of a solution of 3,3'-[(4-Hydroxyphenyl)methyl]bis-(4-hydroxy-2*H*-chromen-2-one) (L10) in ethanol. The crystal structure analysis revealed the formation of L10 · EtOH.

The ORTEP-representation[43] of the molecular structure of L10 · EtOH shown in Figure 2 reveals the successful conversion of the two equivalents of 4-hydroxycoumarin and 4-hydroxybenzaldehyde.

Table 1. Crystal and experimental data

Chemical formula	$C_{27}H_{22}O_8$
Formula weight	474.45
D_x	1.413 Mg m^{-3}
Crystal description	Block, colourless
Crystal size	0.56 × 0.40 × 0.23 mm
Crystal system/Space group	Monoclinic, $P2_1/n$
Temperature	123 K
Unit cell dimensions	
a	11.6867 (4) Å
b	10.1021 (3) Å
c	18.9817 (6) Å
β	95.797 (2)°
V	2229.52 (12) Å^3
Z	4
Absorption coefficient, μ	0.11 mm^{-1}
No. of reflections collected	23737
No. of independent reflections	3918
Data	3515
Goodness of fit on F^2	1.050
R indices [$I < 2\sigma(I)$]:	$R_1 = 0.0298$, w$R_2 = 0.0755$
R indices (all data):	$R_1 = 0.0338$, w$R_2 = 0.0794$
F(000)	992
CCDC deposition no	970314

The interactions of the sterically demanding coumarin units and the 4-hydroxyphenyl fragment – all connected to C1– are indicated by some slightly widened tetrahedral angles of C1 and its connected atoms: (C17C1C8: 112.4°; C17C1C2: 114.0°; C8C1C2: 115.9°). Accordingly, the three angles involving C1 and the remaining straight bonded H1 are slightly smaller than 109.5° of an ideal tetrahedron (all H1C1C2/C8/C17: 104.3°). A complete list of distances and angles are summarized in Table S1 and S2 in the supporting information.

In principle, the keto- and the hydroxy groups of the bis-coumarins are able to form intra- or intermolecular hydrogen bonds (Scheme 1).

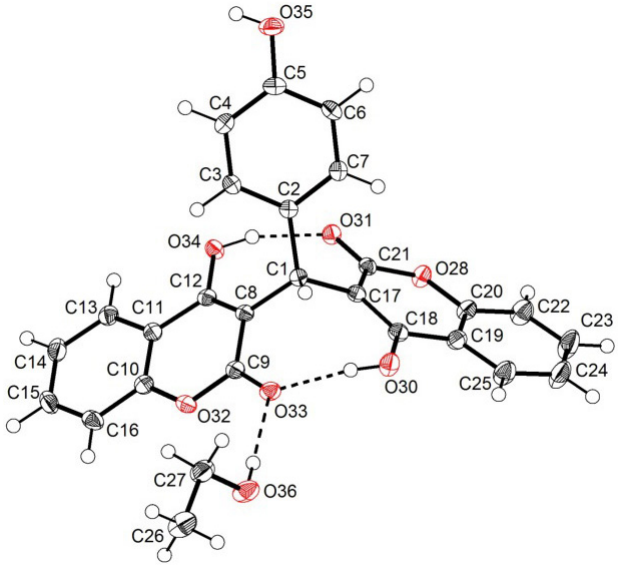

Figure 2. ORTEP-plot with numbering scheme of L10 · ethanol. The displacement ellipsoids are drawn at the 50% probability level; hydrogen atoms are shown as spheres of arbitrary size. Dashed lines represent the hydrogen bonds.

If one bis-coumarin molecule forms two intramolecular hydrogen bonds no interaction with a neighbouring molecule is observed (type i). If one of these bonds is leaved the formation of two intermolecular hydrogen bonds to an adjacent bis-coumarin is possible, and as a consequence, a dimer is formed (type ii). The formation of type i) is realized in the crystal structure of L10 · ethanol and in the previous described isotypic crystal structure of 4-hydroxy-3-[(2-oxo-2H-chromen-3-yl)-(3,4-dihydroxyphenyl)methyl]-chromen-2-one · ethanol.[44] On the other hand type ii) was observed in the ethyl-2-[bis(4-hydroxy-2-oxo-2H-chromen-3-yl)methyl]benzoic acid ester.[45] Bilateral intermolecular hydrogen bonding results in the formation of linear chains (type iii). However, we have not observed this type of bonding so far. As denoted above, in the crystal structure described herein, O30 of the hydroxyl group and O31 of the keto group of one 4-hydroxycoumarin unit of the molecule are intramolecular hydrogen bonded to the keto oxygen O33 and the hydroxy oxygen O34, respectively. Furthermore, the keto oxygen O33 serves as acceptor for the proton of the intermolecular bridging ethanol oxygen O36 from the

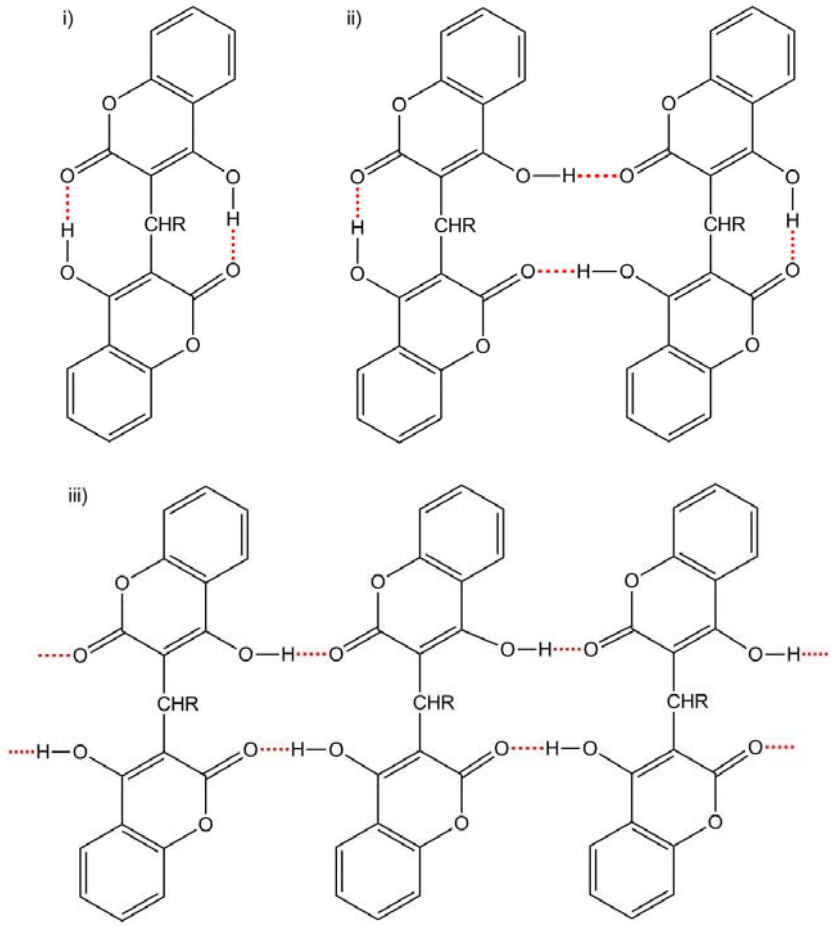

Scheme 1. Formation of two intramolecular hydrogen bonds between the both bis-coumarin units of the investigated molecules (type i). Intra- and intermolecular hydrogen bonding results in the formation of dimers (type ii). Exclusive formation of intermolecular hydrogen bonds between the bis-coumarins of neighbored molecules results in the formation of linear chains (type iii).

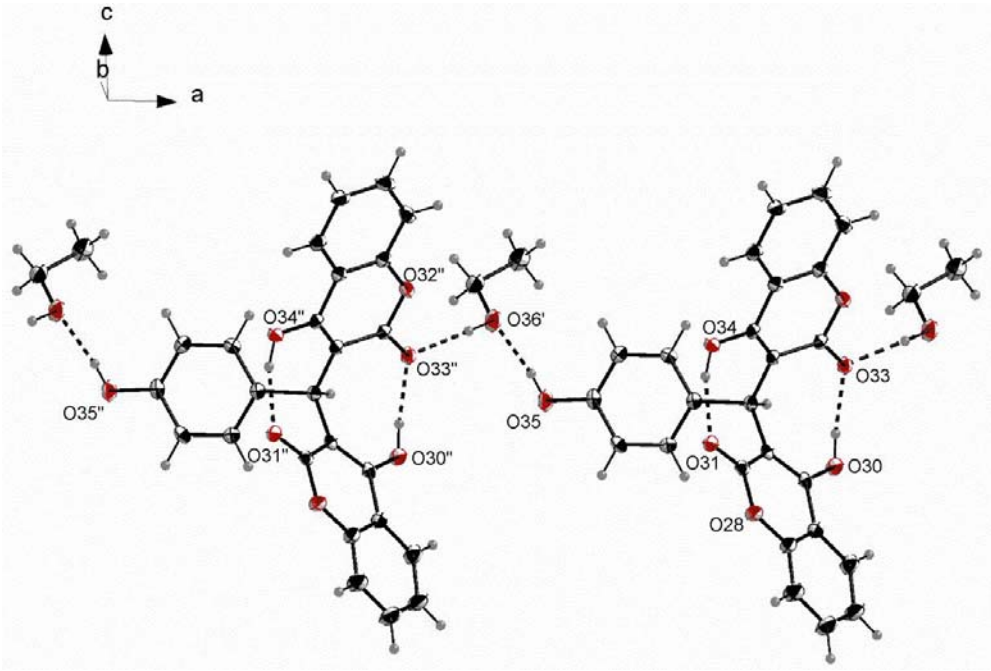

Figure 3. Rendering representation of two hydrogen bonded molecules of L10, with numbering scheme of the participated oxygen atoms. [Symmetry codes: (') 0.5 – x, 0.5 + y, 0.5 – z; (") –1 + x, y, z].

solvent. In turn O36 is an acceptor for H35 of the 4-hydroxyphenyl fragment of the next neighbour molecule. The resulting intra- and intermolecular hydrogen bonds are shown as black dashed lines in Figure 3. The dashed black lines indicate the intramolecular hydrogen bonds between the two coumarin units and the intermolecular hydrogen bonded network of the title compound and the solvent ethanol. The hydroxyl group of a co-crystallized ethanol molecule forms hydrogen bonds with the 4-hydroxyphenyl unit of one molecule and with the keto oxygen O33 of the neighboring bis-coumarin, and by this is forming linear chains in the crystallographic a-direction i.e. EtOH forms bridges between the coumarin molecules. Displacement ellipsoids are drawn at the 50% probability level; H atoms are shown as small spheres of arbitrary size.

This arrangement of the intermolecular hydrogen bonding results in the formation of linear chains based on L10 and ethanol in the crystallographic *a*-direction (Figure 3). The distances and angles of the atoms participated in the hydrogen bonding are summarized in Table 2.

Table 2. Hydrogen bond geometry (Å, °)

D H··· A	D – H	H···A	D···A	D – H···A
O30H30···O33	0.875(13)	1.8432(1)	2.7047(1)	167.97(1)
O34H34···O31	0.873(13)	1.7956(1)	2.6315(1)	159.72(1)
O36' H36'···O33"	0.849(14)	1.9662(1)	2.8116(1)	174.02(1)
O35H35···O36'	0.853(14)	1.8516(1)	2.6969(1)	170.46(1)

Symmetry codes: (') 0.5 – x, 0.5 + y, 0.5 – z; (") –1 + x, y, z.

3. 2. UV-Vis Absorption of L10 Solutions

3. 2. 1. Absorption spectra in individual protic and aprotic solvents

The absorption of L10 was recorded in a number of pure solvents (CH_2Cl_2, CH_3COOH, $CHCl_3$, C_2H_5OH, CH_3OH, CH_3CN, DMF, DMSO) including water even though the solubility of L10 in it is very low. In the studied range (250–350 nm), the solvents do not show UV absorption; EtOH and H_2O showing absorption only below 210 nm and CH_2Cl_2 only below 235 nm.[34] The sol-

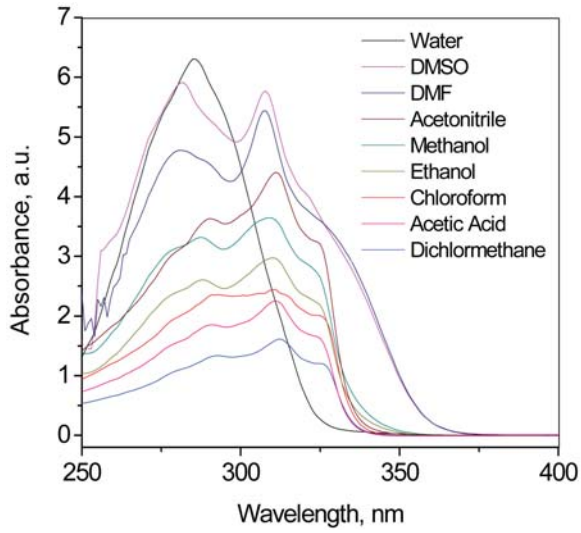

Figure 4. UV spectra of L10 dissolved in different solvents (according the legend, from top to bottom).

vents themselves are suitable for a study of the UV-Vis absorption of L10. Three absorption bands are observed (Figure 4).

The values for λ_{max} for the most intensive absorption bands in the solvents used are presented in Table 3, with dielectric constants given in brackets. In ethanol and methanol solutions, a slight deformation of the absorption curve is visible. In CH_3CN, chloroform and DMF solutions, the band in the interval 300–315 is very clear (for the coumarin 2H-chromen-2-one in CH_3CN, the band at 272 nm is the most intensive[46] instead of that at 311 nm). In protic solvents, with increasing dielectric constant the value of λ_{max} decreases sharply, especially for H_2O. In aprotic solvents there is no clear tendency.

3. 2. 2. Absorption Spectra in Systems of Two Solvents

The UV-Vis absorption of L10, was observed in DMSO/H_2O (ε_{DMSO} = 37.78/ε_{H2O} = 80.4) and CH_2Cl_2/C_2H_5OH (ε_{CH2Cl2} = 9.1/ε_{C2H5OH} = 24.5) two-component systems at different ratios of the aprotic/protic solvents. By varying the solvent ratio, the dielectric constant of the continuum was varied.

In both systems, absorption bands of L10 (two in DMSO/H_2O and three in CH_2Cl_2/C_2H_5OH) were observed in the spectral range 250–350 nm. In the CH_2Cl_2/C_2H_5OH solvent system an absorption band of L10 can be seen in the range of 200–250 nm. (The values of λ_{max} of the absorption bands in the different intervals are given in Table S3 and S4 in the supporting information).

In the DMSO/H_2O system, a shift of the λ_{max} to the shorter wavelengths can be seen with increasing solvent polarity, i.e. with increasing H_2O content (ε = 80.4) vs. DMSO (ε = 37.78) (Figure 5a, Table S3). The same tendency is observed in the CH_2Cl_2/C_2H_5OH solvent system, where small shifts of ± 1 nm to the shorter wavelengths are noticeable (Figure 5b, Table S4).

Three factors influencing the position of λ_{max} in the spectrum of L10 can be pointed out: the solvent polarity, the hydrogen bonding possibilities, and the Lewis base/acid strength of the solvents. They can occur simultaneously. We observed that an increase of the content of the more polar solvent with higher dielectric constant causes a slight hypsochromic shift. This is contrary to expectations because absorption is expected to be shifting to a longer wavelength as the solvent polarity increases.[35,36] However, in water and other hydrogen bonding solvents

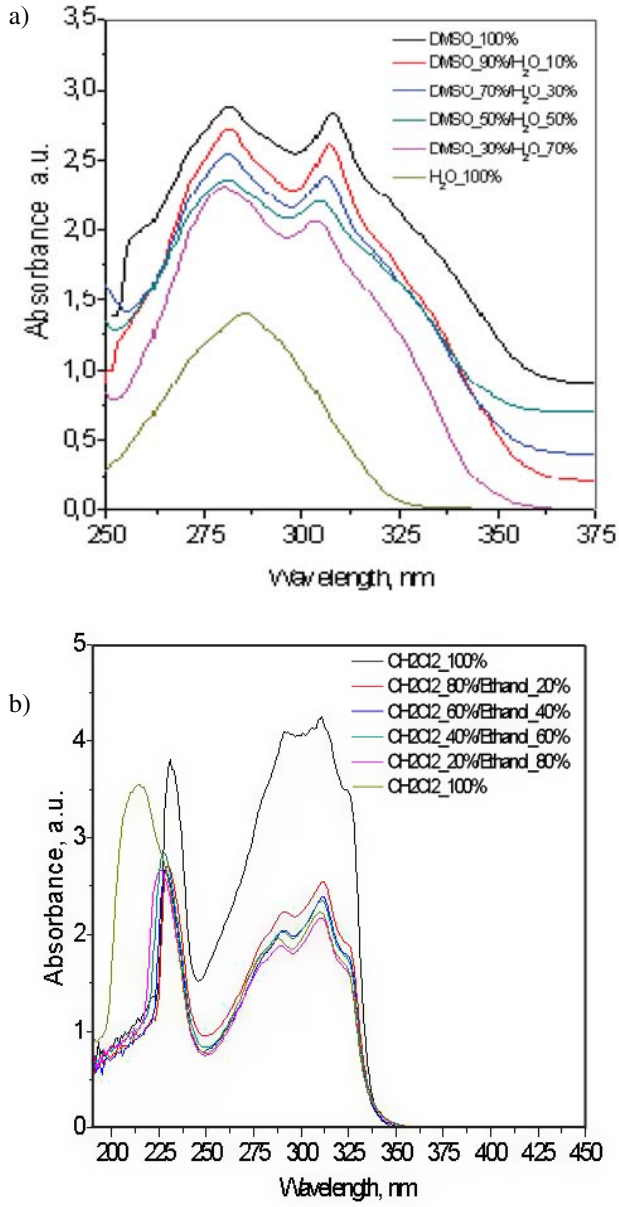

Figure 5. UV spectra of L10 in DMSO/H_2O solution (a) and in CH_2Cl_2/C_2H_5OH solution (b).

such as methanol and ethanol, it is possible to see the opposite effect.[47] This can indicate that a hydrogen bonding effect predominates over solvent polarity effects. In case of L10, the existence of intra-molecular hydrogen bonds between OH groups and –C=O groups of two coumarin fragments is shown on the ORTEP view of the molecular

Table 3. Comparison of the most intensive absorption bands (λmax / nm) of L10 in protic (pr) and aprotic (apr) solvents, arranged by increasing dielectric constant (in brackets).

CH_3Cl	CH_2Cl_2	C_2H_5OH	CH_3OH	DMF	CH_3CN	DMSO	H_2O
$(4.8)_{apr}$	$(9.1)_{apr}$	$(24.3)_{pr}$	$(32.6)_{pr}$	$(36.71)_{apr}$	$(37.5)_{apr}$	$(37.78)_{apr}$	$(80)_{pr}$
306/312	311	311/306	311/309	307	312	308	285

structure (Figure 2, Scheme 1). The third OH group of L10 at the p- position in the phenyl ring is the only one available for hydrogen bonding with H_2O molecules. Apparently it is enough to ensure protonated forms of L10 are formed in water and these cause hypsochromic shift. A competition of solvent polarity and hydrogen bonding in protic solvents has been noticed for some mono-coumarins (like 7,8-dihydroxy-4-methyl-coumarin).[48] In spite of the fact that DMSO, a strong Lewis base, can accept protons and facilitate the deprotonation of L10 (and cause shifts to longer wavelengths),[34] it does not happen here. Apparently the strong hydrogen bondings with L10 formed by the water are dominating over the Lewis base strength of DMSO. A hypsochromic shift may also be caused by a change of the medium or by structural changes like removal of conjugation.

In pure water (Figure 5a, the first curve, from bottom to top; Table S3) the bands observed in the interval 250–350 nm overlap and the λ_{max} at 285 nm of the resulting broad band is closer to the shorter wavelength edge of the interval, suggesting that protonated forms exist. The absorption band of L10 in water has a different structure and position, which is additional evidence for the strong interaction between the L10 and water molecules (ε = 80.4) without deprotonation.

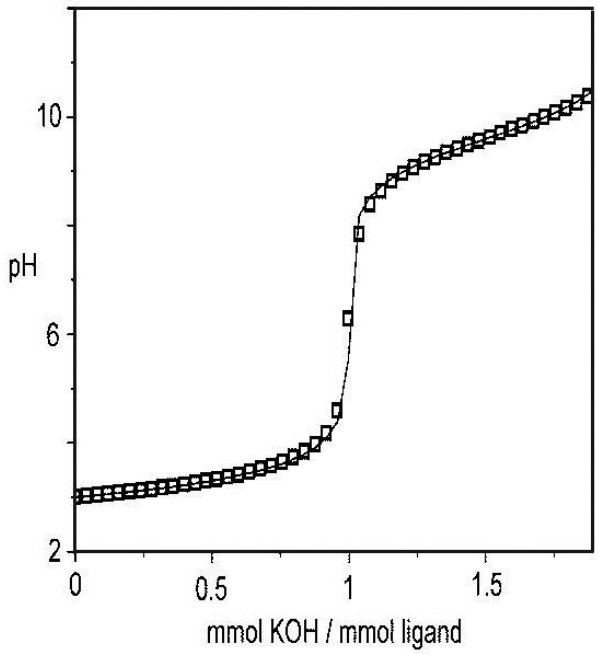

Figure 6. Titration curve of L16 (25 °C, 0.1 M KCl, x_{DMSO} = 0.2). Squares refer to experimental values, the fitting curve was calculated using the formation constants evaluated from the potentiometric measurement.

3. 3. pK_a Determination

Because of the marginal solubility of L10 and L16, potentiometric measurements (μ = 0.1 M KCl, T = 25 °C) were performed in mixtures of DMSO/water using a mole fraction of x_{DMSO} = 0.2. For L10, comparison of the observed experimental data of the back titration experiment (0.1 M HCl) with the titration curve resulted from the titration with 0.1 M KOH, clearly shows the deviation of the both curves indicating the decomposition of the compound during the experiment. ^{1}H-NMR studies of L10 with time under acidic and basic conditions confirm these results (Figure S1). However, for L16 (Figure 6) no decomposition was observed during the titration experiment. (For one more bis-coumarin derivative 3,3'-[(4-Chlorophenyl)methyl] bis-(4-hydroxy-2*H*-chromen-2-one) = L15, potentiometric experiments were performed, too. The degree of decomposition was clearly less pronounced than for L10, but a satisfactory fit of the observed data could not be achieved. Although for pK_{a2} = 10.56, the calculated line overlapped the observed data fairly good, it is noticeable, that the first deprotonation step is finished slightly behind one equivalent of added base/mmol L15 (Figure S2)).

The continuous line fitting the data of the titration curve given in Figure 6 was calculated using the formation constants for the model $L16H_{-1}$ and $L16H_{-2}$, with a pK_{a2} = 9.61(1). This value is in good agreement with a pK_a of 9.8 observed for 3,3'-[(4-hydroxy-3-methoxy-5-nitrophenyl)methyl]bis(4-hydroxy-2*H*-1-benzopyran-2-one) in ethanol.[19] The calculated species distribution given in Figure 7 shows that in the investigated pH range used for the potentiometric experiment the $L16H_{-1}$ species is exclusively formed in the acidic solution, and hence, a pK_{a1} has to be specified < 2. However, the step in the titration curve at one equivalent KOH/mmol L16 clearly indicates the deprotonation of one equivalent L16.

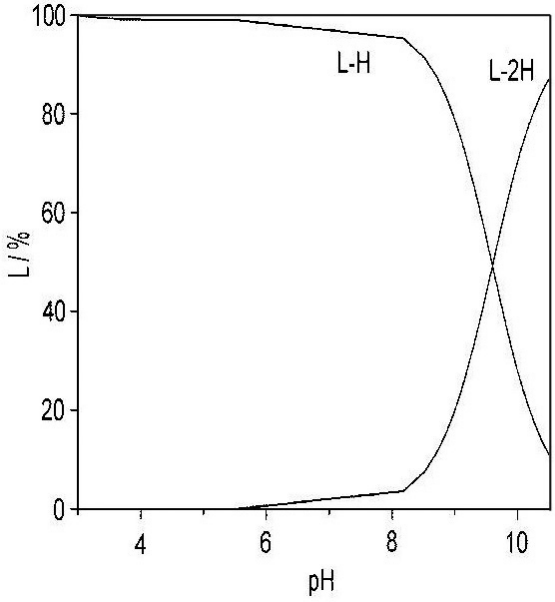

Figure 7. Species distribution of L16 in dependence of pH (25 °C, I = 0.1 M, x_{DMSO} = 0.2). The formation constants evaluated from the potentiometric measurements of L16 were used for the calculations.

Furthermore, even in the DMSO/water mixture no evidence for a deprotonation of the hydroxy group of the 4-hydroxyphenyl unit was found. We cannot explain the large difference between the observed pK_{a1} and pK_{a2} values in detail, but in some extend the interaction of the hydrogen bonding combined with the structural changes and formation of keto-enol tautomerism seems to play the crucial role (see 3.1 and ^{1}H-NMR titration experiments). The comparative low value for pK_{a1} can be explained by the resonance forms of the coumarin carboxylate ion (Scheme S1). The corresponding pK_a value of 4-hydroxycoumarin is 4.10.[49] From the pK_a values found, it is clear that a synthetic procedure to prepare Ln(III) complexes with bis-coumarins at around pH 5 will not allow deprotonation of more than 1 hydroxy group of the 4-hydroxy biscoumarin. This pH will help to avoid formation of lanthanoid hydroxides that are known to precipitate at a pH above 5.5 but complexes with decreasing degree of protonation can be expected to be formed.

To follow the deprotonation steps in more detail, ^{1}H-NMR titration experiments were performed of L16. A sample of L16 was dissolved in DMSO/H_2O (mole ratio 4:1) and different pH* values from 4 to 14.4 were prepared, using KOD and DCl, respectively. ^{1}H-NMR spectra were obtained for each pH and the characteristics of the signals indicating the non labile protons in close proximity to the basic centre of the molecule were studied.

In Figure 8, the development of the spectra with increasing pH is shown. The signal for the methylene group proton at about 6.3 ppm slowly disappears until a pH close to the pKa_2 is reached. At this pH both the single deprotonated L16H$_{-1}$ and the twofold deprotonated L16H$_{-2}$ coexist.

Because the protonation reactions are fast on the NMR-timescale, typically, only one time-averaged signal for the protonated and deprotonated forms are observed in the ^{1}H-NMR spectrum. However, if deprotonation is accompanied with a structural change which is slowly on the NMR-time scale the signals representing the different structures could be both observed.[50] The pK_{a2} value of 10.4 resulting from the ^{1}H-NMR experiment is not in good agreement with a value of 9.61 yielded from the potentiometric titration. However, the different experimental conditions like 0.1 M ionic strength in the potentiometric titration experiment versus the deuterated solvents without using an inert electrolyte, but reading pH* from the pH-meter has to be taken into account. At pH 12.6 the deprotonation has been finished and as a consequence only one signal about 6.0 ppm is observed. The coexistence of precisely two structures is exemplified in the presence of

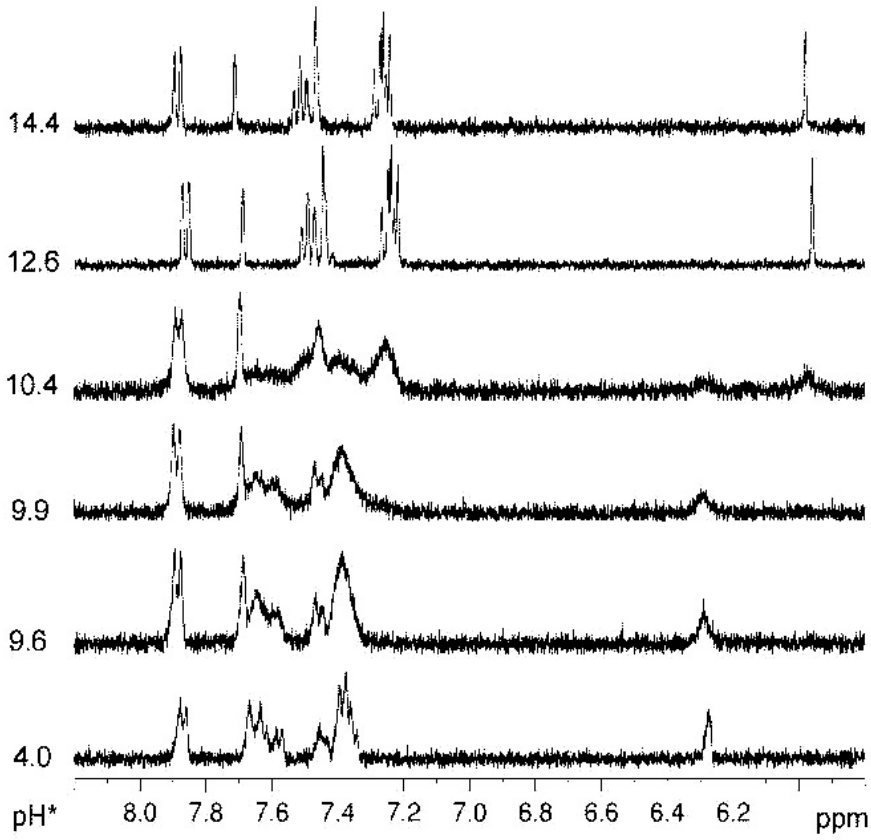

Figure 8. ^{1}H-NMR titration experiments of L16. At pH* = 10.4, obviously two discriminable species could be detected in solution. In contrast, below and above pH* = pK_{a2}, the species L16H$_{-1}$ and L16H$_{-2}$ are formed exclusively in solution.

an isosbestic point observed in the pH dependent UV-vis spectra of L10 in a mixture of ethanol/water discussed in section 3.4. We have no precise explanation for the visual nature of the two structures before and after the conversion, but it is well known that conformational change and keto-enol tautomery can be observed at such structures. Similar ^{1}H-NMR spectra were recorded with time (Figure S1) for L10, at pH 2.4 and 13. Here, the increasing of new signals with time (marked with asterisks) is an indication for the decomposition of L10 in acidic, as well as in the basic pH range. Nevertheless, as for L16 a significant shift for the methylene group proton H1 is observed at high pH.

3. 4. UV-vis Titration Experiments

Besides the determination of the pK_a values for some bis-coumarins with potentiometric and ^{1}H-NMR spectroscopy a UV-Vis titration experiment for L10 was performed. A solution of L10 with a concentration of 1.10^{-4} M in 1/9 (v/v) C_2H_5OH/H_2O (23.2–23.7 °C) was prepared and spectra with increasing pH were measured. The UV-Vis absorption spectra at pH 2.00 up to 11.30 are given in Figure 9.

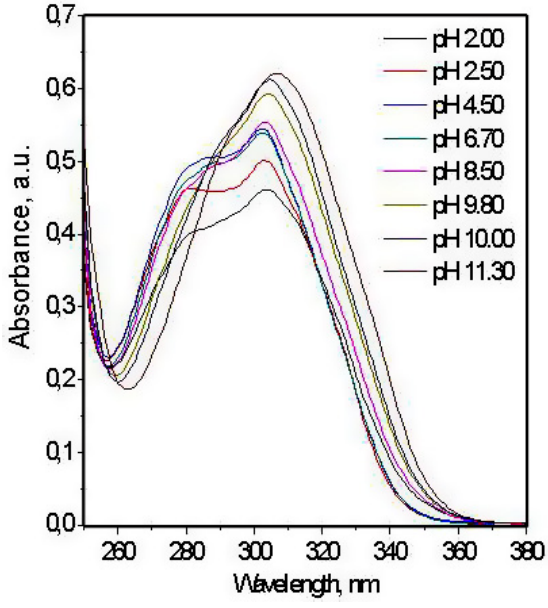

Figure 9. UV-Vis absorption spectra of L10 solutions (1.10^{-4} M, C_2H_5OH/H_2O), depending on pH.

Up to pH = 6.70 the increasing pH only influences the amount of the absorbance, but at pH = 8.5, pH = 9.80 and pH = 10.00 the spectra clearly run through an isosbestic point. At this point, exact two species, namely $L10H_{-1}$ and $L10H_{-2}$ are presented in solution. It is clear, that the equimolar ratios of $L10H_{-1}$ and $L10H_{-2}$ together with the corresponding pH value result in the pK_{a2}, but however, because of the known decomposition of L10 in aqueous solution no exact value can be given. However, at pH = 11.30 the isosbestic point exists no longer and only $L10H_{-2}$ is present in solution. Taking this into account, an estimated value for pK_{a2} of 9.5 ± 1 is by all means realistic.

4. Conclusions

The formation of 3,3'-[(4-Hydroxyphenyl)methyl] bis-(4-hydroxy-2*H*-chromen-2-one) · C_2H_5OH was revealed by the crystal structure analysis. Hydrogen bonds both intramolecular in the bis-coumarin units and intermolecular between the title compound and the solvent ethanol are observed. The hydroxyl group of a co-crystallized ethanol molecule connects a 4-hydroxyphenyl unit of one molecule with the keto oxygen of the neighbored bis-coumarin, forming linear chains.

The absorption spectra of the solutions of L10 in solvents with increasing polarity and dielectric constants demonstrate a hypsochromic shift which is most pronounced for water. This can be explained by the predomination of hydrogen bonding effect over the solvent polarity effects. The existence of the isosbestic point in the pH interval 8.5–10.00 can be connected with the deprotonated species $L10H_{-1}$ and $L10H_{-2}$, presented in solution.

The results from the research done show that the compound L10 has low stability with the time in DMSO/H_2O solutions as well as in strongly acidic or basic solutions. The comparison with a similar system L16, which is stable in the investigated pH range shows, that such bis-coumarins can be twofold deprotonated with pK_{a1} values < 2 and a pK_{a2} in the basic region about pH 10.

The fluorescent spectrum of L10 (λ_{ex} 250 nm) was found to be typical for coumarins, which often absorb in the UV and emit in the blue light.[46,51] The maximum in the spectrum of the powdered sample is at 424 nm (Figure S3).

5. Acknowledgements

The financial support from the Bulgarian Fund for Scientific Investigations (Contract DO 02-129/08) as well as the Contract for mutual cooperation between the University of Sofia and Saarland University are gratefully acknowledged.

6. References

1. B. D. Wagner, *Molecules*, **2009,** *14,* 210–237.
2. H. Zhao, N. Neamati, H. Hong, A. Mazumder, S. Wang, S. Sunder, G. W. A. Milne, Y. Pommier, T. R. Burke, *J. Med. Chem.* **1997,** *40,* 242–248.
3. A. H. Bedair, N. A. El-Hady, M. S. A. El-Latif, A. H. Fakery, A. M. El-Agrody, *Il Farmaco,* **2000,** *55,* 708–714.

4. F. Chimenti, D. Secci, A. Bolasco, P. Chimenti, A. Granese, O. Befani, P. Turini, S. Alcaro, F. Ortuso, *Bioorg. Med. Chem. Lett*. **2004,** *14,* 3697–3703.
5. I. Kostova, *Curr. HIV Res.* **2006,** *4(3),* 347–363.
6. D. Završnik, S. Muratović, S. Špirtović, D. Softić, M. Medić-Šarić, *Bosnian J, Basic Med. Sci*. **2008;** *8(3),* 277–281.
7. D. Završnik, S. Muratović, D. Makuc, J. Plavec, M. Cetina, A. Nagl, E. De Clercq, J. Balzarini, M. Mintas, *Molecules* **2011,** *16,* 6023–6040.
8. D. Završnik, S. Spirtovic-Halilovic, D. Softic, *Period. Biol.* **2011,** *113(1),* 93–97.
9. L. Wu, X. Wang, W. Xu, F. Farzaneh, R. Xu, *Curr. Med. Chem.* **2009,** *16,* 4236–4260.
10. S. Stanchev, G. Momekov, F. Jensen, I. Manolov, *Eur. J. Med. Chem.* **2008,** *43(4),* 694–706.
11. I. Manolov, C. Maichle-Moessmer, N. Danchev, *Eur. J. Med. Chem.* **2006,** *41,* 882–890.
12. S. Stanchev, V. Hadjimitova, T. Traykov, T. Boyanov, I. Manolov, *Eur. J. Med. Chem.* **2009,** *44,* 3077–3082.
13. C. Su, J. Mouscadet, C. Chiang, H. Tsai, L. Hsu, *Chem. Pharm. Bull.* **2006,** *54(5)* 682–686.
14. H. E. Katerinopoulos, *Curr. Pharm. Des.* **2004,** *10(30),* 3835–3852.
15. C. Chih-Chia, H. Ling-Yih, T. Hou-Jen, Y. Chen-Wen, C. Tsu-Chung, *J.C.C.I.T.* **2008,** *37(1)* 15–21.
16. R. E. Gallan, M. Laferriere, J. C. Scaiano, *J. Mater. Chem.* **2006,** *16,* 1697–1701.
17. K. J. Wallace, R. I. Fagbemi, F. J. Folmer-Andersen, J. Morey, V. M. Lynth, E. V. Anslyn, *Chem. Commun.* **2006,** *37,* 3886–3888.
18. J. Motoyanagi, T. Fukushima, N. Ishii, T. Aida*, J. Am. Chem. Soc.* **2006,** *128(13)*, 4220–4221.
19. S. Stanchev, C. Maichle-Mössmer, I. Manolov, *Z Naturforsch* **2007,** *62b*, 737–741.
20. B. Karmakara, A. Nayak, J. Banerji, *Tetr. Letters* **2012,** *53(33)*, 4343–4346.
21. P. Singh, P. Kumar, A. Katyal, R. Kalra, S. K. Dass, S. Prakash, R. Chandra *Catalysis Lett.* **2010,** *134 (3–4)*, 303–308.
22. I. Manolov, C. Maichle-Moessmer, *Analyt. Sci*. **2007,** *23,* x63–x64.
23. I. Manolov, M. Ströbele, H.-J. Meyer, *Analyt. Sci. – X-ray Struct. Anal. Online* **2008,** *24(7),* 135–136.
24. S. Stanchev, A. Penkova, P. Retailleau, G. Avdeev, I. Manolov, *X-ray Struct. Anal. Online* **2008,** *24(9),* 183–4.
25. J. Yao, W. Dou, W. Liu, J. Zheng, *Inorg. Chem. Comm*. **2009,** *12,* 430–432.
26. N. Ravikumar, G. Gopikrishna, K. A. Solomon, *Acta Cryst. Section E*, **2012,** *E68,* o265.
27. L. V. Chang-Wei, Y.-P. Wu, J. Liu, J. I. A. Xin-Gang, *Chinese J. Struct. Chem*. **2012,** *31(6),* 847–850.
28. I. Kostova, N. Trendafilova, G. Momekov, *J. Inorg. Biochem.* **2005,** *99,* 477–87.
29. I. Kostova, I. Manolov, I. Nikolova, N. Danchev, *Il Farmaco* **2001,** *56,* 707– 711.
30. I. Kostova, I. Manolov, G. Momekov, *Eur. J. Med. Chem.* **2004,** *39,* 765–775.
31. I. Kostova, I. Manolov, G. Momekov, Tz. Tzanova, S. Konstantinov, M. Karaivanova, *Eur. J. Med. Chem.* **2005,** *40,* 1246–1254.
32. R. H. Goodwin, B. M. Pollock, *Arch. Biochem. Biophys.* **1954,** *49(1),* 1–6.
33. L. Xie, Y. Chen, W. Wu, H. Guo, J. Zhao, X. Yu, *Dyes and Pigments* **2012,** *92,* 1361–1369.
34. B. D. Mistry, A handbook of spectroscopic data: Chemistry (UV, IR, PMR, 13CNMR and Mass Spectroscopy), Jaipur: Oxford Book Company, **2009**.
35. G. J. Smith, C. L. Dunford, P. B. Roberts, *J. Photochem. Photobiol. A: Chemistry* **2010,** *210,* 31–35.
36. J. Donovalová, M. Cigáň, H. Stankovičova, J. Gašpar, M. Danko, A. Gáplovský, P. Hrdlovič, *Molecules* **2012,** *17,* 3259–3276.
37. a) G. M. Sheldrick SHELX97. Program for the Refinement of Crystal Structures from Diffraction Data, University of Göttingen, Germany, 1997. b) G. M. Sheldrick, *Acta Cryst*. **2008,** *A64,* 112–122.
38. J. T. W. Lai, F. W. Lau, D. Robb, P. Westh, G. Nielson, C. Trandum, A. Hvidt, Y. Koga, *J. Solution Chem.* **1995,** *24,* 89–102.
39. P. Gans, A. Sabatini, A. Vacca, *Talanta* **1996,** *43,* 1739–1753.
40. S. Steinhauser, U. Heinz, M. Bartholomä, T. Weyhermüller, H. Nick, K. Hegetschweiler, *Eur. J. Inorg. Chem.* **2004,** *21,* 4177–4192.
41. Bruker. *APEX2*, *SAINT* and *SADABS*. Bruker AXS Inc., Madison, Wisconsin, USA, **2010**.
42. P. Müller, R. Herbst-Irmer, A. L. Spek, T. R. Schneider, M. R. Sawya, Crystal Structure Refinement – A Crystallographer's Guide to SHELXL, Oxford University Press, *2006*.
43. K. Brandenburg "DIAMOND", Crystal Impact GbR. Bonn, Germany, *2011*.
44. I. Manolov, B. Morgenstern, K. Hegetschweiler, *X-ray Struct. Anal. Online* **2012,** *28,* 87–88.
45. I. Manolov, B. Morgenstern, K. Hegetschweiler, *X-ray Struct. Anal. Online* **2012,** *28*, 83–84.
46. R. M. Christie, C. H. Lui, *Dyes and Pigments* **1999**, *42,* 85–93.
47. O. K. Abou-Zied, O. I. K. Al-Shihi, *Proc. of SPIE* **2008,** 6867:68670K-1-12.
48. B. H. M. Hussein, *J. Lumin.* **2011,** *131,* 900–908.
49. V. P. Georgievskii, *Khimiya Prirodnykh Soedinenii* **1985,** *6*, 770–73.
50. C. Neis, D. Petry, A. Demangeon, B. Morgenstern, D. Kuppert, J. Huppert, S. Stucky, K. Hegetschweiler, *Inorg. Chem.* **2010,** *49*, 10092–10107.
51. T. N. Kopylova, L. G. Samsonova, R. M. Gadirov, V. P. Khilya, V. V. Ishchenko, O. V. Shablykina, in: Atomic and Molecular Pulsed Lasers VII, ed. V. F. Tarasenko*. Proc. of SPIE* **2007,** 6938:6938G1–G6.

Povzetek

Spojino 3,3'-[(4-hidroksifenil)metil]bis-(4-hidroksi-2*H*-kromen-2-on) smo pripravili s pomočjo Knoevenaglove reakcije. Kristale, primerne za rentgensko difrakcijsko analizo, smo vzgojili s pomočjo počasnega izhlapevanja etanola. Produkt 3,3'-[(4-hidroksifenil)metil]bis-(4-hidroksi-2*H*-kromen-2-on) · etanol je kristaliziral v monoklinskem sistemu, skupina $P2_1/n$. Ultravijolični/vidni absorpcijski spekter smo posneli v različnih topilih. Opazovali smo občutljivost spojin na polarnost topila in prisotnost vodikovih vezi s protičnimi (etanol, voda) in aprotičnimi topili (dimetilsulfoksid, acetonitril). Glede na ^{1}H-NMR spektroskopske rezultate in potenciometrične ter UV/VIS tritracijske eksperimente smo ocenili kislinske disociacijske konstante za 3,3'-[(4-hidroksifenil)metil]bis-(4-hidroksi-2*H*-kromen-2-on).

Supplementary data

Synthesis, Crystal Structure and Physico-chemical Properties of 3,3'-[(4-hydroxyphenyl)methyl] bis-(4-hydroxy-*2H*-chromen-2-one)

Denitsa Elenkova, Bernd Morgenstern, Ilia Manolov and Maria Milanova

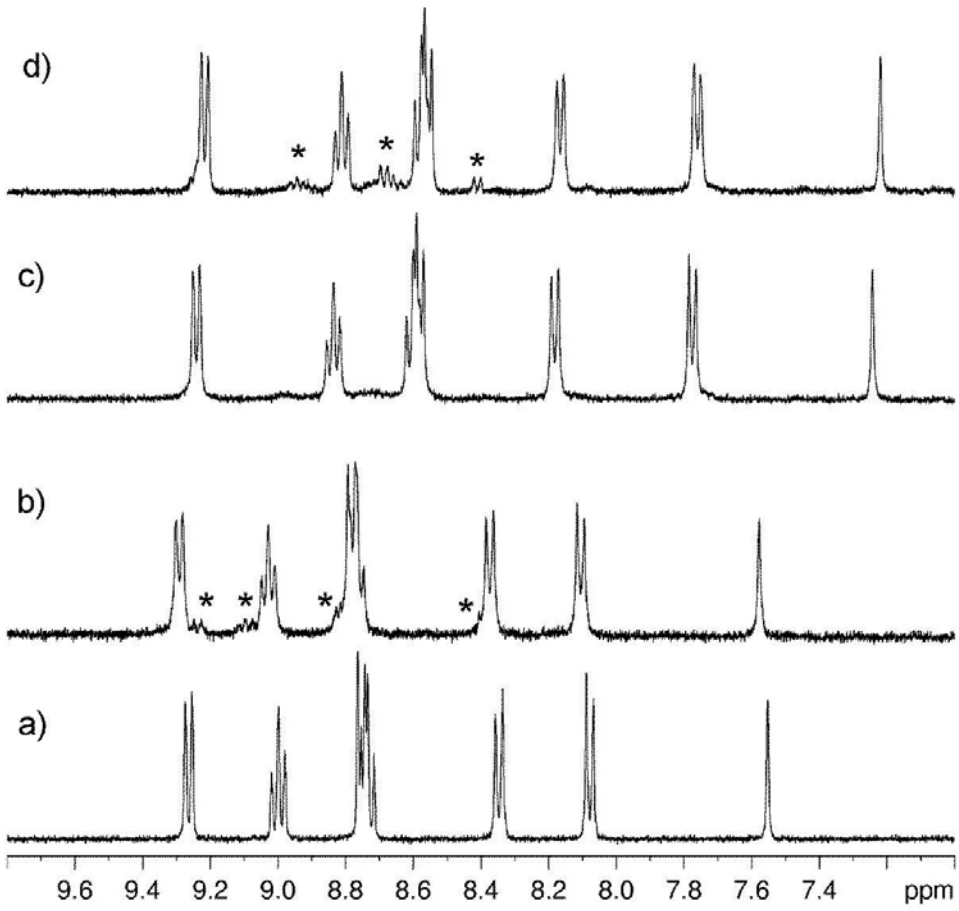

Figure S1. NMR titration of L10 at different values of pH, respectively pH = 2.4 fresh, 13 fresh, 13 fresh after 30 min, 2.4 after 30 min, from bottom to top.

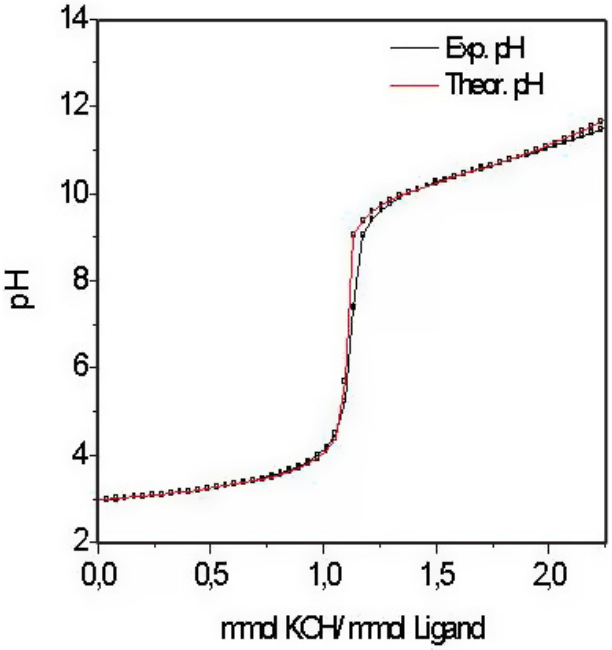

Figure S2. Potentiometric titration curve of L15.

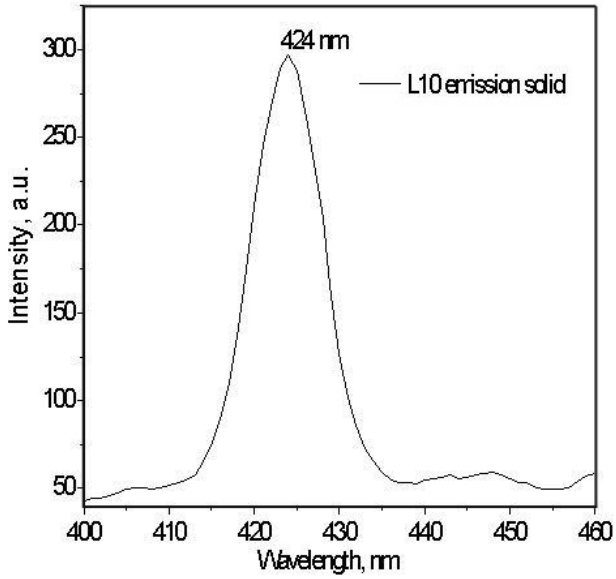

Figure S3. Emission spectrum of L10 (λ_{ex} 250 nm).

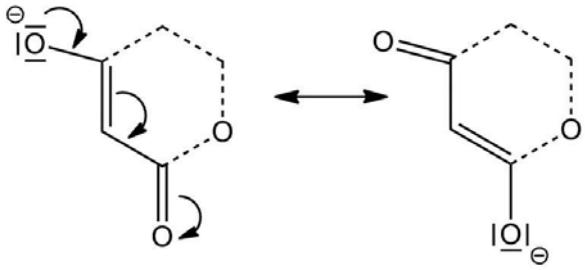

Scheme S1. Resonance forms of coumarin fragment, which resemble the carboxylate ion.

Table S1. Bond lengths [Å] for L10 · ethanol.

C(1)-C(8)	1.5180(16)	C(15)-H(15)	0.9500
C(1)-C(17)	1.5207(16)	C(16)-H(16)	0.9500
C(1)-C(2)	1.5297(16)	C(17)-C(18)	1.3640(17)
C(1)-H(1)	1.0000	C(17)-C(21)	1.4372(17)
C(2)-C(3)	1.3888(17)	C(18)-O(30)	1.3390(15)
C(2)-C(7)	1.3944(16)	C(18)-C(19)	1.4456(18)
C(3)-C(4)	1.3903(17)	C(19)-C(20)	1.3908(18)
C(3)-H(3)	0.9500	C(19)-C(25)	1.3990(18)
C(4)-C(5)	1.3911(18)	C(20)-O(28)	1.3801(15)
C(4)-H(4)	0.9500	C(20)-C(22)	1.3835(19)
C(5)-O(35)	1.3584(15)	C(21)-O(31)	1.2257(14)
C(5)-C(6)	1.3875(18)	C(21)-O(28)	1.3657(15)
C(6)-C(7)	1.3829(17)	C(22)-C(23)	1.380(2)
C(6)-H(6)	0.9500	C(22)-H(22)	0.9500
C(7)-H(7)	0.9500	C(23)-C(24)	1.390(2)
C(8)-C(12)	1.3622(17)	C(23)-H(23)	0.9500
C(8)-C(9)	1.4384(16)	C(24)-C(25)	1.376(2)
C(9)-O(33)	1.2354(15)	C(24)-H(24)	0.9500
C(9)-O(32)	1.3518(14)	C(25)-H(25)	0.9500
C(10)-O(32)	1.3739(15)	C(26)-C(27)	1.494(2)
C(10)-C(16)	1.3857(18)	C(26)-H(26A)	0.9800
C(10)-C(11)	1.3881(17)	C(26)-H(26B)	0.9800
C(11)-C(13)	1.4002(18)	C(26)-H(26C)	0.9800
C(11)-C(12)	1.4452(16)	C(27)-O(36)	1.4260(17)
C(12)-O(34)	1.3338(14)	C(27)-H(27A)	0.982(17)
C(13)-C(14)	1.3769(18)	C(27)-H(27B)	1.003(18)
C(13)-H(13)	0.9500	O(30)-H(30)	0.875(13)
C(14)-C(15)	1.396(2)	O(34)-H(34)	0.873(13)
C(14)-H(14)	0.9500	O(35)-H(35)	0.853(14)
C(15)-C(16)	1.377(2)	O(36)-H(36)	0.849(14)

Table S2. Bond angles [°] for L10 • ethanol.

C(8)-C(1)-C(17)	112.35(9)	C(15)-C(16)-C(10)	118.71(12)
C(8)-C(1)-C(2)	115.94(10)	C(15)-C(16)-H(16)	120.6
C(17)-C(1)-C(2)	114.03(9)	C(10)-C(16)-H(16)	120.6
C(8)-C(1)-H(1)	104.3	C(18)-C(17)-C(21)	119.21(11)
C(17)-C(1)-H(1)	104.3	C(18)-C(17)-C(1)	122.36(11)
C(2)-C(1)-H(1)	104.3	C(21)-C(17)-C(1)	118.43(10)
C(3)-C(2)-C(7)	117.48(11)	O(30)-C(18)-C(17)	123.61(11)
C(3)-C(2)-C(1)	122.38(10)	O(30)-C(18)-C(19)	115.63(11)
C(7)-C(2)-C(1)	119.52(10)	C(17)-C(18)-C(19)	120.72(11)
C(2)-C(3)-C(4)	121.53(11)	C(20)-C(19)-C(25)	118.34(12)
C(2)-C(3)-H(3)	119.2	C(20)-C(19)-C(18)	117.56(11)
C(4)-C(3)-H(3)	119.2	C(25)-C(19)-C(18)	124.04(12)
C(3)-C(4)-C(5)	120.11(11)	O(28)-C(20)-C(22)	116.86(11)
C(3)-C(4)-H(4)	119.9	O(28)-C(20)-C(19)	121.09(11)
C(5)-C(4)-H(4)	119.9	C(22)-C(20)-C(19)	122.06(12)
O(35)-C(5)-C(6)	117.34(11)	O(31)-C(21)-O(28)	115.33(10)
O(35)-C(5)-C(4)	123.72(11)	O(31)-C(21)-C(17)	125.33(11)
C(6)-C(5)-C(4)	118.93(11)	O(28)-C(21)-C(17)	119.33(10)
C(7)-C(6)-C(5)	120.39(11)	C(23)-C(22)-C(20)	118.48(13)
C(7)-C(6)-H(6)	119.8	C(23)-C(22)-H(22)	120.8
C(5)-C(6)-H(6)	119.8	C(20)-C(22)-H(22)	120.8
C(6)-C(7)-C(2)	121.56(11)	C(22)-C(23)-C(24)	120.68(13)
C(6)-C(7)-H(7)	119.2	C(22)-C(23)-H(23)	119.7
C(2)-C(7)-H(7)	119.2	C(24)-C(23)-H(23)	119.7
C(12)-C(8)-C(9)	118.90(11)	C(25)-C(24)-C(23)	120.37(13)
C(12)-C(8)-C(1)	126.47(10)	C(25)-C(24)-H(24)	119.8
C(9)-C(8)-C(1)	114.60(10)	C(23)-C(24)-H(24)	119.8
O(33)-C(9)-O(32)	115.58(10)	C(24)-C(25)-C(19)	120.05(13)
O(33)-C(9)-C(8)	124.17(11)	C(24)-C(25)-H(25)	120.0
O(32)-C(9)-C(8)	120.24(10)	C(19)-C(25)-H(25)	120.0
O(32)-C(10)-C(16)	116.75(11)	C(27)-C(26)-H(26A)	109.5
O(32)-C(10)-C(11)	121.32(11)	C(27)-C(26)-H(26B)	109.5
C(16)-C(10)-C(11)	121.92(12)	H(26A)-C(26)-H(26B)	109.5
C(10)-C(11)-C(13)	118.47(11)	C(27)-C(26)-H(26C)	109.5
C(10)-C(11)-C(12)	117.88(11)	H(26A)-C(26)-H(26C)	109.5
C(13)-C(11)-C(12)	123.64(11)	H(26B)-C(26)-H(26C)	109.5
O(34)-C(12)-C(8)	124.76(11)	O(36)-C(27)-C(26)	108.38(11)
O(34)-C(12)-C(11)	115.12(10)	O(36)-C(27)-H(27A)	110.2(10)
C(8)-C(12)-C(11)	120.08(11)	C(26)-C(27)-H(27A)	111.7(10)
C(14)-C(13)-C(11)	120.10(12)	O(36)-C(27)-H(27B)	109.1(10)
C(14)-C(13)-H(13)	120.0	C(26)-C(27)-H(27B)	109.7(10)
C(11)-C(13)-H(13)	120.0	H(27A)-C(27)-H(27B)	107.7(13)
C(13)-C(14)-C(15)	120.22(12)	C(21)-O(28)-C(20)	121.35(9)
C(13)-C(14)-H(14)	119.9	C(18)-O(30)-H(30)	110.4(11)
C(15)-C(14)-H(14)	119.9	C(9)-O(32)-C(10)	120.77(9)
C(16)-C(15)-C(14)	120.56(12)	C(12)-O(34)-H(34)	111.5(10)
C(16)-C(15)-H(15)	119.7	C(5)-O(35)-H(35)	108.3(12)
C(14)-C(15)-H(15)	119.7	C(27)-O(36)-H(36)	109.1(12)

Table S3. Absorption of L10 in DMSO/H_2O solutions; λ_{max} in the different intervals

	DMSO/Water (v/v)	**100/0**	**90/10**	**70/30**	**50/50**	**30/70**	**0/100**
1	λ_{max}, nm (interval 250–290 nm)	282	282	281	281	281	285
2	λ_{max}, nm (interval 290–350 nm)	308	307	306	305	304	

Table S4. Absorption of L10 in CH_2Cl_2/C_2H_5OH solution; λ_{max} in the different intervals

	CH_2Cl_2/C_2H_5OH	**100/0**	**80/20**	**60/40**	**40/60**	**20/80**	**0/100**
1	interval 300–320 nm λ_{max} = (311 ± 1) nm	311	312	312	311	310	310
2	interval 250–300 nm λ_{max} = (290 ± 1) nm	291	291	290	290	288	288
3	interval 315–330 nm λ_{max} (sh.) = (325 ± 1) nm	324	325	326	324	324	324
4	interval 200–250 nm	231	229	229	228	226	214